



JAAS

Rapid, Quantitative, and Non-destructive SR-WD-XRF Mapping of Trace Platinum in Byzantine Roman Empire Gold Coins

| | |
|-------------------------------|-------------------------------------------------------------------------------------------------------------------------------------------------------------------------------------------------------------------------------------------------------------------------------------------------------------------------------------------------------------------------------------------------------------------------------------------------------------------------------------------------------------------------|
| Journal: | <i>Journal of Analytical Atomic Spectrometry</i> |
| Manuscript ID | JA-ART-07-2018-000227.R1 |
| Article Type: | Paper |
| Date Submitted by the Author: | 11-Aug-2018 |
| Complete List of Authors: | Van Loon, Lisa; University of Western Ontario, Anthropology; University of Western Ontario, Earth Sciences; Numismatic Institute of North America Inc Banerjee, Neil; University of Western Ontario, Earth Sciences; Numismatic Institute of North America Inc Hinds, Michael; Royal Canadian Mint, Assay Gordon, Robert; Simon Fraser University, Physics Bevan, George; Queens University, Department of Classics Burgess, Richard; University of Ottawa, Department of Classics and Religious Studies |
| | |

SCHOLARONE™
Manuscripts



Journal Name

ARTICLE

Rapid, Quantitative, and Non-destructive SR-WD-XRF Mapping of Trace Platinum in Byzantine Roman Empire Gold Coins

Lisa L. Van Loon,^{a,b,c} Neil R. Banerjee,^{b,c} Michael W. Hinds,^d Robert Gordon,^e George Bevan,^f and R. W. Burgess^g

Received 00th January 20xx,
Accepted 00th January 20xx

DOI: 10.1039/x0xx00000x

www.rsc.org/

Non-destructive analytical techniques that enable the rapid screening of large numbers of coins are of interest for numismatic studies. Using a tuneable synchrotron X-ray source provides an intensity that cannot be matched by laboratory X-ray fluorescence (XRF) sources, reduces analytical time and increases sample throughput. Here we evaluate the combination of the high intensity and spatial resolution provided by a synchrotron source with the highly resolved sensitivity afforded by a wavelength dispersive (WD) spectrometer for the rapid, quantitative, and non-destructive XRF mapping of trace platinum in ancient Roman gold coins. In this study, the rapid mapping of >3300 data points in (400 μm x 400 μm) areas was done to determine Pt distribution across the gold coin matrix. Quantitative analysis was performed by using gold reference materials with known platinum concentrations. The results of this study agree within -11 – +3% of previously determined trace platinum concentrations in these gold coins. The application of this method will enable researchers to quickly screen large numbers of ancient coins for classification and comparison for further analysis.

Introduction

Interest in the identification of rapid, non-destructive methods for the analytical examination of metal cultural artefacts is increasing.¹⁻⁴ In the case of ancient numismatic objects, non-destructive analytical techniques have been of interest for several decades.⁵ Along with being non-destructive, desired techniques for the study of ancient artefacts should also be fast, versatile, and sensitive.¹ In the case of numismatics, an ideal method would enable researchers to quickly screen large numbers of ancient coins for classification and comparison of coins for further analysis.^{3,6}

Synchrotron radiation X-ray fluorescence (SR-XRF) is well-suited to the investigation of metal artefacts, including numismatic objects, to provide clues about their

manufacturing and origin of materials.^{1,3,7-10} First, SR-XRF does not require a piece of the artifact be removed for analysis, so valuable objects are not damaged. Secondly, a synchrotron source offers high brilliance that is not matched by laboratory XRF sources. This enables fast data collection with a high signal to noise ratio. Third, SR-XRF provides the high spatial resolution necessary for studying the distribution of non-homogeneous trace elements within an object. Finally, the excitation energy selected using a synchrotron source can be tuned to optimize conditions for data collection and to improve the detection of trace elements by minimizing the signal from a major matrix element (e.g., gold in coins). Together, these properties make SR-XRF an excellent choice for rapid, sensitive, and accurate non-destructive micro-analysis.

The use of a wavelength dispersive (WD) detector for SR-XRF analysis provides improved resolution and lower detection limits over more common energy dispersive (ED) detectors.^{6,12} For the study of gold objects, such as coins, WD detectors can provide the energy resolution needed to distinguish the signal of a trace element like platinum (atomic number 79) in an overwhelming gold matrix (atomic number 80). Additionally, with appropriate standards, quantitative analyses can be performed using WD-XRF.^{12,13}

The trace elements associated with gold can serve as a fingerprint of its original source. In particular, these fingerprints are being used in archaeometry to identify the

^a Western University, Department of Anthropology, London, ON Canada. E-mail: lisa.vanloon@uwo.ca

^b Western University, Department of Earth Sciences, London, ON Canada. E-mail: neil.banerjee@uwo.ca

^c Numismatic Institute of North America Inc., London, ON. E-mail: numismatics.institute@gmail.com

^d Royal Canadian Mint, 320 Sussex Dr., Ottawa, ON, K1A 0G8, Canada. Email: hinds@mint.ca

^e Simon Fraser University, Department of Physics, Burnaby, BC Canada. E-mail: ragordon@alumni.sfu.ca

^f Queens University, Department of Classics, 510 Watson Hall, Kingston, ON, K7L 3N6, Canada. Email: George.bevan@gmail.com

^g University of Ottawa, Department of Classics and Religious Studies, 55 Laurier Ave, Ottawa, ON, K1N 6N5, Canada. Email: rburgess@uottawa.ca

origin and manufacturing of historical gold objects.^{3,7,14,15} Platinum is known to associate with native gold¹⁶ and is commonly used as a tracer for gold provenance and manufacturing.² With a melting point >700 °C above that of gold [1064 °C], trace amounts of Pt may have remained intact during ancient manufacturing, and so, trace Pt found in these artefacts is associated with a primary gold source.²

Changes in the concentration of trace elements, such as Pt, indicate changes in either the material source or in manufacturing techniques.^{2,17,18} For this reason, the quantitative analysis of trace platinum associated with gold objects is important in archaeological and historical research. In particular the Pt concentration in gold coins minted during the fourth century Byzantine Roman Empire increases significantly, suggesting new sources of gold became available.¹⁷

A previous study¹⁷ evaluated laboratory (400W Rh tube) wavelength dispersive XRF analysis to quantitatively determine the concentration of trace platinum in a nearly pure gold matrix. A suite of coins from the Byzantine Roman Empire were selected for comparative analysis. The coins were polished on one side to remove impressed design and create a flat surface needed for Spark Ablation Inductively Coupled Plasma Optical Emission Spectrometry (SA-ICP-OES) and lab XRF analysis. The concentrations measured by WD-XRF agreed with SA-ICP-OES, within 13%. A non-contact and non-destructive method for measuring Pt in ancient gold was developed. However, due to the low flux available, long collection times were required to measure the low Pt concentrations. With the large spot size for the measurement, both elevated and depressed areas were measured on the impressed side, leading to an observed low concentration bias on the impressed side. A correction was proposed for the depth of the coin's elevated decoration

Here we evaluate the combination of the high brilliance and spatial resolution provided by a synchrotron source with the highly resolved detection afforded by a WD spectrometer for the rapid and quantitative analysis of trace platinum in gold coins manufactured in the Byzantine Roman Empire.

Experimental

Three gold coins minted in the Byzantine Roman Empire were selected for quantitative Pt analysis using SR-XRF combined with a wavelength dispersive detector. The coins were part of a previous study and are labelled #2, #3, and #6, Figure 1.¹⁷ For all three coins, one side had been polished flat. Three gold reference materials (CHL A, CHL B, CHL C) were obtained from the Royal Canadian Mint Assay Department. These standards were developed to assess the purity of gold from 98.4% to 99.99% and contain known concentrations of nine trace elements, including Pt. All materials were analyzed as

received. Prior to measurement, the surfaces were wiped with methanol.

Data Collection

Data collection was performed at the Advanced Photon Source at Beamline 20ID (Argonne National Laboratory, Lemont, IL).¹⁹ The energy was selected using a Si(111) monochromator. The flux at 10 keV is 10^{12} photons/sec/mm² for the 5 μm microbeam. The energy resolution of the beamline (1.3×10^{-4} keV) is essentially limited by the natural width of the Si(111) monochromator. Data collection was performed with a Microspec WDX wavelength dispersive spectrometer with a LiF (200) analyzer crystal and two built-in gas proportional counters operated simultaneously.²⁰ The measured signal was converted into pulses and counted. The measured current amplitude was converted into pulses and counted. The count rate was kept below 10,000 counts per second to minimize deadtime issues in the gas proportional detector. The recorded signal was normalized to the incident flux, I₀, prior to any analysis, and is reported as Normalized Signal (A.U.).

Pt distribution maps (400 μm x 400 μm) were created by rastering in the x and y directions in 7 μm steps using a dwell time of 300 msec per point. The size of the mapped area was chosen to be similar to the spot size of a single LA-ICP-MS measurement, since it is a well-known technique for the study of historical artefacts.²¹ Four maps were collected on the polished side of each coin and four maps were collected on flat regions of the imprinted side of each coin. On Coin #2, four maps were collected on four structured regions of the imprinted side. Maps were collected on each reference material and care was taken to select clean areas.

Data analysis

Maps of Pt distribution were created using the 2D ScanPlot software at Beamline 20ID. XANES data was processed using the Athena software program.²² Calibration of the energy position was done by collecting a Pt foil spectrum. The collected XANES spectrum was calibrated at the Pt L₃ edge to 11564 eV. The spectrum was background-corrected by subtracting a straight line fit to the pre-edge from the entire spectrum. The spectra were normalized by using a straight line fit to the post edge region of the XANES spectrum. All additional analyses were performed using Origin 2017 (OriginLab, Northampton, MA) and Microsoft Excel.

Selection of SR excitation energy and WD collection wavelength

The WD collection wavelength region from 1.28 – 1.38 Å was scanned using five different excitation energies to determine the best combination of excitation X-ray energy and XRF WD collection wavelength to discriminate the Pt L α signal from the gold X-ray Raman related background. Figure 2 shows SR-WD-XRF scans at five different excitation energies, and the fluorescence signal in the Pt and Au L α regions. The collection wavelength was set for the Pt L α XRF emission line at 1.313 Å (9442.5 eV). An excitation energy of 11580 eV (Pt L₃ = 11564

eV) was selected to collect the best Pt signal while minimizing contribution from the Au Raman background. To confirm that the Pt signal was maximized and real, the Pt L₃ XANES region was scanned from -200 eV to 16 k relative to the Pt edge with an integration time of 2 sec/point, Figure 3, and a metallic Pt spectrum was observed.²³

Results and discussion

SR-WD-XRF analysis of platinum in RCM gold reference materials.

The Pt concentrations in the three Royal Canadian Mint (RCM) reference materials are 600 ppm (CHL A; 98.379% Au), 300 ppm (CHL B; 99.244% Au), and 12 ppm (CHL C; 99.926% Au). The reference materials chosen were within the range of the expected Pt concentrations in the three coins. Four unique SR-WD-XRF (400 μm x 400 μm) maps were collected as replicates for each reference material, Figure 4. Each data point was collected with a dwell time of 300 msec. The maps show that Pt is evenly distributed in the reference materials. An average value for the normalized signal (A.U.) was obtained for each map, Table 1. A Pt calibration curve was prepared, Figure 5, and a least-squares equation was obtained to determine trace Pt concentrations in a gold matrix, Equation (1):

$$\text{ppm}_{\text{Pt}} = (\text{Normalized Signal}_{1.313} - 2.22 \times 10^{-4}) / (4.36 \times 10^{-6} / \text{ppm}) \quad (1)$$

The calibration curve shows a linear response in this concentration range measured, indicating that the SR-WD-XRF analysis is suitable for the quantitative determination of trace Pt concentrations in Byzantine Roman Empire gold coins.

SR-WD-XRF analysis of platinum in Byzantine coins

Four unique (400 μm x 400 μm) SR-WD-XRF maps were collected as replicates on the polished side of each coin and are shown in Figure 6. Four flat regions were selected on the imprinted side of each coin for analysis and are shown in Figure 7. Additionally, four raised areas on the imprinted side of Coin #2 were selected for analysis and are shown in Figure 8. With SR-WD-XRF microprobe mapping, the variation in Pt distribution is revealed. The determined Pt concentration for each mapped area is reported in Table 2. The averaged Pt concentrations with standard errors for the polished and imprinted sides of each coin are reported in Tables 3 and 4. The maps shown in Figure 6 - 8 show the variation in Pt distributions that is reflected in the standard deviations reported in Table 1.

The polished side of Coin #2 is fairly uniform and the four mapped areas had little variation in Pt concentrations or in standard deviations, suggesting that Pt is evenly distributed in the coin. Coin #6 showed greater variation than Coin #2 but again, the standard deviations reported for each mapped area are similar, indicating that the Pt is evenly mixed in the gold matrix. Coin #3 showed variation in Pt concentration and in

standard deviations. The maps revealed hot spots of high Pt concentration within the (400 μm x 400 μm) areas.

Pt distribution and concentrations determined on polished sides of the coins.

The Pt distribution measured on the polished side of Coin #2 is homogeneous, with little variation in Pt concentrations or in standard deviations. The Pt distribution measured for Coin #6 showed greater variation than Coin #2 but again, the standard deviations are similar, suggesting that the Pt is evenly mixed in the gold matrix. The determined Pt concentrations on the polished sides of Coins #2 and #6 are (285 ± 17) ppm and (290 ± 11) ppm, respectively. Coin #3 showed variation in Pt concentration and in standard deviations. The maps revealed hot spots of high Pt concentration within the mapped areas. The hotspots are reflected in the reported standard error for the determined Pt concentration of (424 ± 75) ppm

Pt distribution and concentrations determined on imprinted sides of the coins.

Pt distribution and concentrations measured on imprinted sides. Four maps were collected on flat sections of the imprinted sides of each coin. Due to the small spot size used, small areas could be selected with minimal scatter from structured areas on the same surface. For each coin, the average Pt concentrations and standard deviations are similar between areas. Coin #2 had a Pt concentration of (302 ± 10) ppm with the smallest standard error, suggesting that Pt is evenly distributed. Coin #6 had a Pt concentration of (303 ± 17) ppm. The measured variation is again greatest for Coin #3 with a Pt concentration of (363 ± 19) ppm. Less variation was observed in these four areas than in the four areas measured on the polished surface. Four maps were collected on structured regions (i.e. beard and crown) on the imprinted side of Coin #2. Due to the small spot size, each measurement can be considered to be on a pseudo-flat surface. The measured Pt concentration is (309 ± 22) ppm

Comparison of polished and imprinted sides.

Pt concentrations were measured on both the polished and imprinted sides of the coins. For Coin #2, the measured average Pt concentration on the polished side was (285 ± 17) ppm. On the imprinted side, the average Pt concentration measured for the flat regions was (302 ± 10) ppm and for the structured regions was (309 ± 22) ppm. For Coin #3, the measured average Pt concentration on the polished side was (424 ± 75) ppm, which reflects the presence of a Pt hotspot in Map 3. On the imprinted side, the average Pt concentration measured for the flat regions was (364 ± 19) ppm. For Coin #6, the measured average Pt concentration on the polished side was (290 ± 12) ppm. On the imprinted side, the average Pt concentration measured for the flat regions was (303 ± 17) ppm. Coins #2 and #6 have similar Pt concentrations and both had lower concentrations on their polished sides than on the imprinted sides. This may suggest differences between Pt concentrations at the surface of the coins (imprinted side) vs. the interior of the coins (polished side). Coin #3 was unique in that maps collected on the polished side showed Pt hotspots,

Figure 5, and the determined Pt concentrations on both the polished and imprinted sides were higher than the concentrations determined for the other coins. This indicates that the Pt concentration is not consistent within the coin. One possibility is that this may be due to nature of the starting material melted (with large particles of platinum in the gold). The reference materials were made by dispersing Pt (< 74 µm diameter particles) in molten gold. If the platinum were in larger particulate form then a more even distribution may not be possible. More coins must be analysed and further study must be done before more inferences can be made.

Comparison with SA-ICP-OES results.¹⁷ The measured SA-ICP-OES results reported in Reference 17 are used for comparison to determine if SR-WD-XRF can be used to measure trace platinum concentrations in gold coins. The measured concentrations are compared in Tables 3 and 4. Overall, the SR-WD-XRF measurements trend in the same general way as the WD-XRF and SA-ICP-OES measurements for the same coins. The results obtained in this work differ by -11 – +3% from the reported SA-ICP-OES measurements. Only Coin #3 had a higher measured Pt concentration on the polished side when compared with the reported SA-ICP-OES measurements. This suggests that the SR-WD-XRF measurement has a low biased Pt measurement, when compared to SA-ICP-OES.

Coin #3 had the highest concentration of Pt, determined by all methods used in this work and previous.¹⁷ The maps collected for Coin #3 on the polished side showed significant variation in the Pt distribution with hot spots observed in two of the maps, which cannot not be measured by either SA-ICP-OES (spot size 1 mm²) or lab XRF (spot size 12 mm²) measurements. This variation suggests that there is segregation or non-uniform distribution of Pt in the gold used for manufacturing, or that the heat used in manufacturing was sufficient to melt gold but insufficient to distribute Pt evenly in Coin #3. Analysis of additional coins should be performed to better understand the differences in Pt distribution.

Conclusions

SR-WD-XRF is a non-destructive, rapid analytical technique for the quantitative analysis of trace elements in a gold matrix. This study evaluated the quantitative analysis of trace Pt in gold Byzantine coins by SR-WD-XRF. An important advantage of SR-WD-XRF is the available flux and non-destructive nature of the measurement. Here, maps with <3300 measurement data points were collected in less than 20 minutes with each data point collected in 300 msec. As well as providing a quantitative Pt concentration, microprobe SR-WD-XRF mapping reveals variation in the spatial distribution of Pt within a single coin.

SR-WD-XRF provides quantitative results when using standards with a similar matrix. Using three gold reference materials, SR-WD-XRF analysis was able to quantitatively

measure the Pt concentration in gold coins from the Byzantine Roman Empire. Results were compared with previously determined Pt concentrations for the same coins and found to agree within -11 – +3%. In addition, the same trends in concentration between coins were observed. Together, these results indicate that SR-WD-XRF can be used to quantitatively measure trace Pt in a gold coin matrix.

The small spot size available from the synchrotron source permitted the determination of Pt concentrations on imprinted surfaces, meaning that the analysis can be performed non-destructively. With the spatial resolution of the synchrotron source, Pt hotspots were observed in Coin #3 that indicate the presence of Pt inclusions. This inhomogeneity cannot be captured with traditional bulk measurement analytical techniques and can be used to gain additional insight into differences between source materials and minting practices.

The ability to non-destructively and rapidly, quantitatively determine trace element concentrations within a gold matrix indicates that SR-WD-XRF is a suitable analytical technique for numismatics. Application of this method will enable researchers to quickly screen large numbers of ancient coins for classification and comparison for further analysis.

Conflicts of Interest

There are no conflicts to declare.

Acknowledgements

We thank the Western University Statistical and Actuarial Sciences Help Desk for consultations. Sector 20 facilities at the Advanced Photon Source, and research at these facilities, are supported by the US Department of Energy - Basic Energy Sciences, the Canadian Light Source and its funding partners, the University of Washington, and the Advanced Photon Source. Use of the Advanced Photon Source, an Office of Science User Facility operated for the U.S. Department of Energy (DOE) Office of Science by Argonne National Laboratory, was supported by the U.S. DOE under Contract No. DE-AC02-06CH11357.

Notes and references

- 1 M. L. Young, Rep. Prog. Phys., 2012, 75.
- 2 A. Adriaens, Spectrochim. Acta B, 2005, 60, 1503-1516.
- 3 M. F. Guerra, X-ray Spectrom., 2008, 37, 317-327.
- 4 B. Newbury, B. Stephenson, J. Almer, M. Notis, G. S. Cargill, G. B. Stephenson, and D. Haeffner, Powder Diff., 2004, 19, 12-15.
- 5 A. Charalambous, Analytical methods for the determination of the chemical composition of ancient coins.
- 6 L. Bertrand, M. Thoury and E. Anheim, J. Cult. Herit., 2013, 14, 277-289.
- 7 M. F. Guerra and T. Calligaro, Meas. Sci. Technol., 2003, 2003, 1527-1537.

Journal Name

ARTICLE

- 1
2
3
4
5
6
7
8
9
10
11
12
13
14
15
16
17
18
19
20
21
22
23
24
25
26
27
28
29
30
31
32
33
34
35
36
37
38
39
40
41
42
43
44
45
46
47
48
49
50
51
52
53
54
55
56
57
58
59
60
- 8 A. Vasilescu and B. Constantinescu, *Rom. Rep. Phys.*, 2011, 63, 901-911.
 - 9 L. Bertrand, M. Cotte, M. Stampanoni, M. Thoury, F. Marone and S. Schoder, *Phys. Rep.*, 2012, 519, 51-96.
 - 10 B. Constantinescu, D. Cristea-Stan, A. Vasilescu, R. Simon and D. Ceccato, *P. Rom. Acad. A*, 2012, 13, 19-26.
 - 11 M. Kavčič, in *X-ray Spectroscopy*, In Tech, 2012, pp. 81-94.
 - 12 F. He and P. J. Van Espen, *Analytical Chemistry*, 1991, 63, 2237-2244.
 - 13 C. N. Zwicky and P. Lienemann, *X-Ray Spectrometry*, 2004, 33, 294-300.
 - 14 M. Radtke, U. Reinholz and H. Riesemeier, *ArcheoSciences. Revue d'archéométrie*, 2009, 39-44.
 - 15 M. F. Guerra, T. Calligaro, M. Radtke, I. Reiche and H. Riesemeier, *Nucl. Instrum. Meth. B*, 2005, 240, 505-511.
 - 16 R. S. Jones, and M. Fleischer. *Gold in minerals and the composition of native gold*. No. 612. [US Dept. of the Interior, Geological Survey], 1969.
 - 17 M. W. Hinds, G. Bevan and R. W. Burgess, *J. Anal. At. Spectrom.*, 2014, 29, 1799-1805.
 - 18 M. Tetland, J. Greenough, B. Fryer, M. Hinds, M. Shaheen, *Geostand. Geoanal. Res.*, 2017, 41, 689-700.
 - 19 S. M. Heald, E. A. Stern, D. Brewer, R. Gordon, D. Crozier, D. Jiang, J. O. Cross, XAFS at the Pacific Northwest Consortium-Collaborative Access Team Undulator Beamline, *J. Synchrotron Rad.*, 2001, 8, 342-344.
 - 20 J. O. Cross, S. M. Heald, Recycling a Wavelength-dispersive Spectrometer for Synchrotron Microprobe EXAFS.
 - 21 L. Dussubieux, L. Van Zelst, *Appl. Phys. A*, 2004, 79, 353-356.
 - 22 B. Ravel, M. Newville, *J. Synchr. Rad.*, 2005, 12, 537-541.
 - 23 Reference X-Ray Spectra of Metal Foils, Exafs Materials, http://exafsmaterials.com/Ref_Spectra_0.4MB.pdf, (accessed July 25, 2017).

Table 1. Average measurement* of Pt L α intensity obtained by SR-WD-XRF for each (400 μ m x 400 μ m) mapped region collected for the three RCM gold reference materials CHL C, B, and A.

| | | Average Pt L α Normalized Signal x 10 ³ (A.U.) | | | |
|-------|---------|------------------------------------------------------------------|-----------------|-----------------|-----------------|
| | Pt, ppm | Map 1 | Map 2 | Map 3 | Map 4 |
| CHL C | 12 | 0.28 \pm 0.06* | 0.28 \pm 0.06 | 0.28 \pm 0.06 | 0.28 \pm 0.06 |
| CHL B | 300 | 1.5 \pm 0.1 | 1.6 \pm 0.1 | 1.5 \pm 0.1 | 1.5 \pm 0.1 |
| CHL A | 600 | 2.8 \pm 0.3 | 2.8 \pm 0.3 | 2.9 \pm 0.3 | 2.8 \pm 0.2 |

* Average values with one standard deviation

Table 2. Average Pt concentrations* for each (400 μm x 400 μm) mapped region on the polished and imprinted side of Coins #2, 3, and 6.

| | | Polished side | | Imprinted side | |
|---------|-------|----------------|--------------|----------------|--------------------|
| | | Pt (ppm) | | Flat Regions | Structured Regions |
| Coin #2 | Map 1 | 271 \pm 59 | 298 \pm 57 | 305 \pm 54 | |
| | Map 2 | 282 \pm 56 | 293 \pm 56 | 250 \pm 60 | |
| | Map 3 | 253 \pm 44 | 331 \pm 47 | 349 \pm 68 | |
| | Map 4 | 237 \pm 56 | 287 \pm 49 | 332 \pm 59 | |
| Coin #3 | Map 1 | 378 \pm 70 | 339 \pm 72 | | |
| | Map 2 | 255 \pm 69 | 323 \pm 81 | | |
| | Map 3 | 613 \pm 1161 | 394 \pm 68 | | |
| | Map 4 | 450 \pm 104 | 398 \pm 73 | | |
| Coin #6 | Map 1 | 323 \pm 69 | 311 \pm 75 | | |
| | Map 2 | 283 \pm 66 | 298 \pm 61 | | |
| | Map 3 | 267 \pm 60 | 259 \pm 52 | | |
| | Map 4 | 285 \pm 44 | 343 \pm 75 | | |

*Average values \pm one standard deviation

Table 3. Average Pt concentrations* measured on the polished sides of Coins #2,3, and 6 in this study and from Hinds *et al*, 2014.¹⁷

| | SR-WD-XRF (ppm) | SA-ICP-OES (ppm) ¹⁷ | Difference (ppm) | % Difference** |
|---------|-----------------|--------------------------------|------------------|----------------|
| Coin #2 | 285 ± 17 | 318 ± 4 | -33 | -10 % |
| Coin #3 | 424 ± 75 | 410 ± 16 | 14 | 3 % |
| Coin #6 | 290 ± 12 | 314 ± 14 | -24 | -8 % |

*Reported values are the average of the values in Table 2 ± standard error.

Standard Error = (Standard Deviation of n maps)/(√n)

**% Difference was calculated as [(SR-WD-XRF)-(SA-ICP-OES)/(SA-ICP-OES)]*100.

Table 4. Pt concentrations* measured on the imprinted sides of Coins #2,3, and 6 in this study and in Hinds *et al*, 2014.¹⁷

| | SR-WD-XRF | SA-ICP-OES ¹⁷ | Difference | % Difference** |
|--------------------|-----------|--------------------------|------------|----------------|
| Flat Regions (ppm) | | | | |
| Coin #2 | 302 ± 10 | 318 ± 4 | -16 | -5 % |
| Coin #3 | 364 ± 19 | 410 ± 16 | -46 | -11 % |
| Coin #6 | 303 ± 17 | 314 ± 14 | -11 | -4 % |
| Structured Regions | | | | |
| Coin #2 | 309 ± 22 | 318 ± 4 | -9 | -3 % |

*Reported values are the average of the values in Table 2 ± standard error.

Standard Error = (Standard Deviation of n maps)/(√n)

**% Difference was calculated as [(SR-WD-XRF)-(SA-ICP-OES)]/(SA-ICP-OES)*100.



Figure 1. The three gold coins analysed in this study. They are solidi of Sear types 959 and 960 from the mint in Constantinople between 13 April 654 and 2 June 659, showing the Byzantine emperors Constans II and Constantine IV. Care was taken not to make measurements in areas marked by SA-ICP-OES on the polished sides.

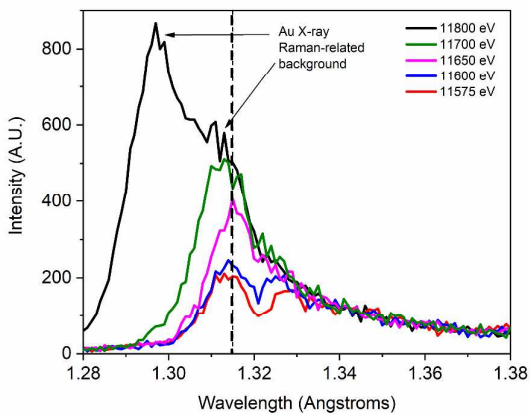


Figure 2. SR-WD XRF signal in the Pt and Au L α regions for five different excitation X-ray energies. An excitation energy of 11580 eV was selected to maximize Pt signal while minimizing the Au X-ray Raman related background. At 11600 eV the Pt L α is distinguishable from the Au X-ray Raman related background. Above 11600 eV the Pt L α signal is hidden by the dominant the Au X-ray Raman related background. The dotted line is a guide to the selected WD collection wavelength of 1.313 Å.

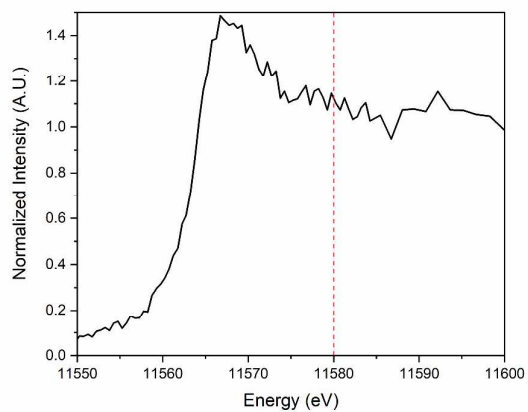


Figure 3. Platinum L3-edge XANES spectrum obtained from the reference material CHL A. The WD detector was set at 1.313 Å. The dotted line is a guide to the selected excitation energy of 11580 eV used for all Pt measurements.

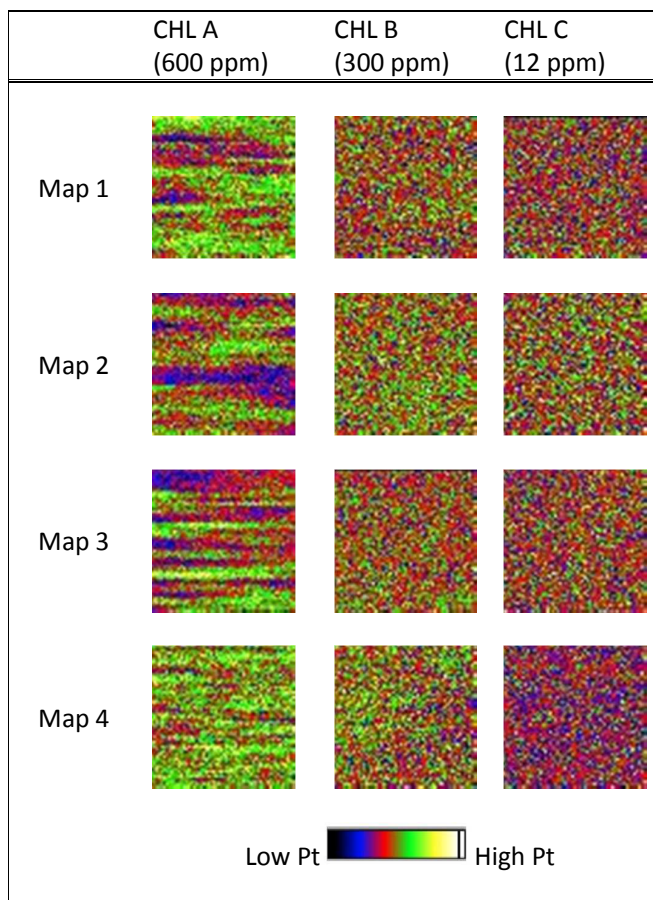


Figure 4. Distribution of Pt in the RCM Au reference materials. Each map is (400 μm x 400 μm). The relative platinum concentrations are represented using a colour scale from white (highest Pt) to black (lowest Pt). The variation in colour reflects the standard deviations reported in Table 1. The maps show that platinum is well-mixed in the gold matrix.

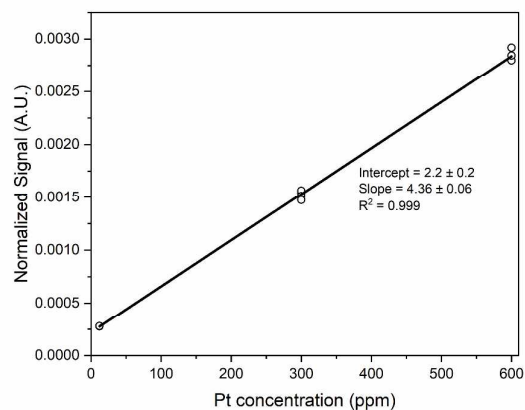


Figure 5. Line of best fit of the intensity of the WD signal measured as a function of Pt concentration for the three RCM reference materials, CHL A, B, and C. The determined intercept and slope were used to calculate Pt concentrations in the three coins.

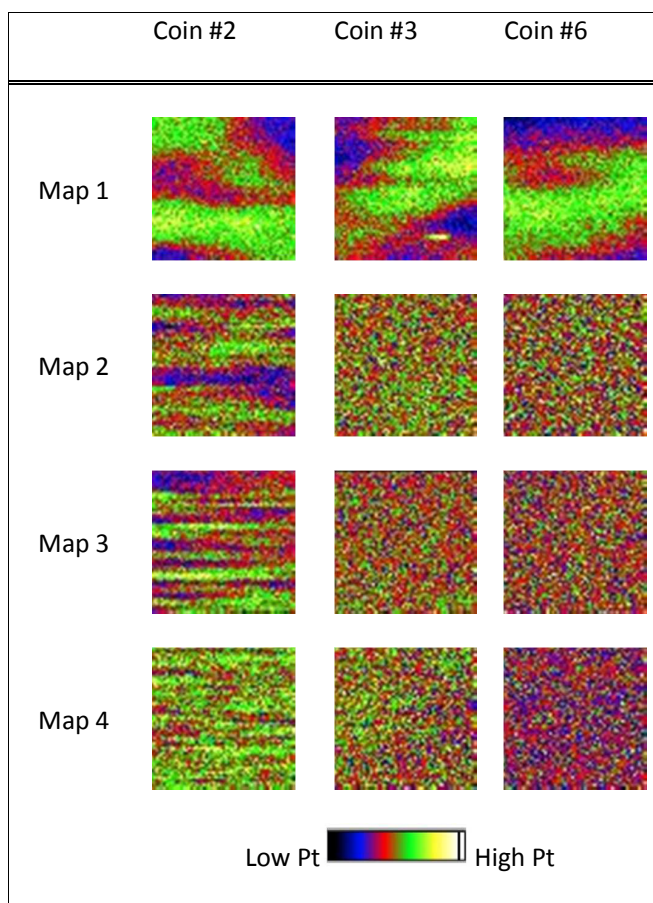


Figure 6. Distribution of Pt in mapped regions on the polished sides of the coins. Each map is (400 μm x 400 μm) except for Coin #6 Map 4 which is (400 μm x 393 μm). The relative platinum concentrations are represented using a colour scale from white (highest Pt) to black (lowest Pt). The variation in colour reflects the standard deviations reported in Table 2. Maps 1 and 3 for Coin 3 show platinum hotspots.

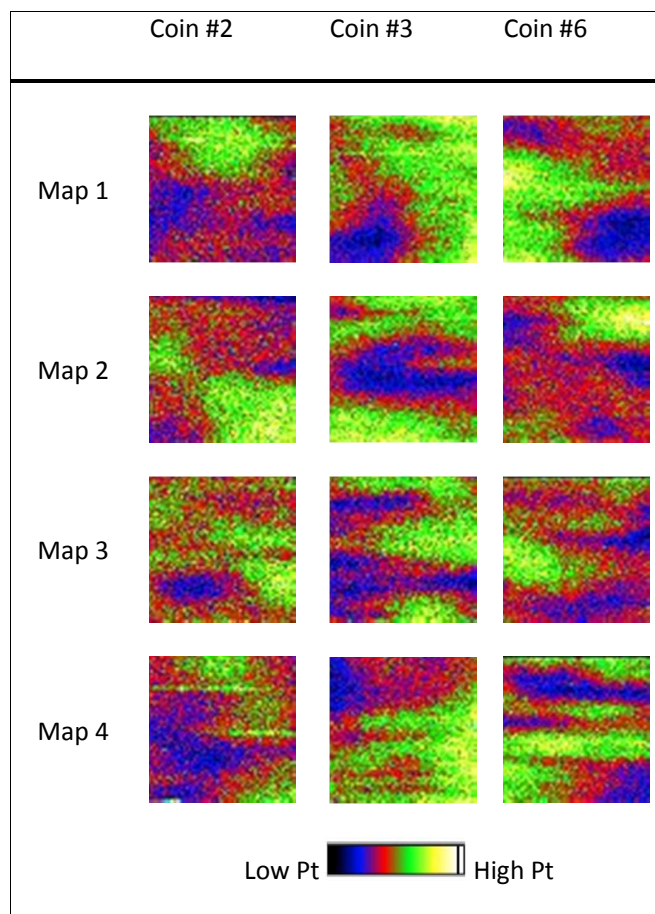


Figure 7. Distribution of Pt in selected flat regions on the imprinted sides of the coins. Each map is (400 μm x 400 μm) except Coin #2 Map 1 and Coin #6 Maps 3 and 4 that are (400 μm x 393 μm). The relative platinum concentrations are represented using a colour scale from white (highest Pt) to black (lowest Pt). The variation in colour reflects the standard deviations reported in Table 2.

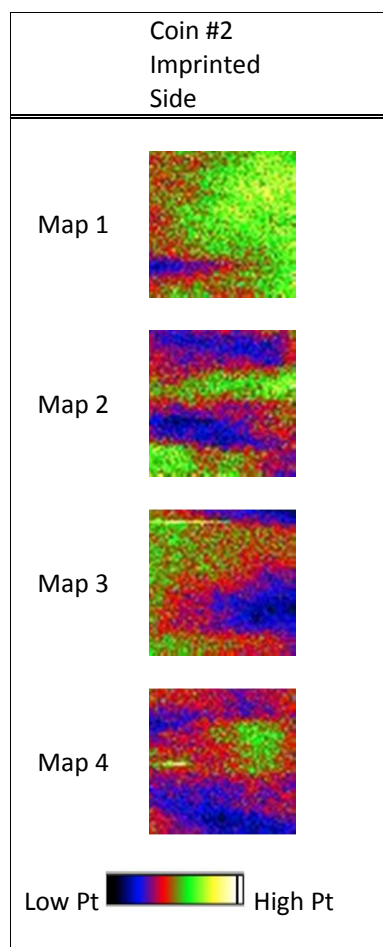
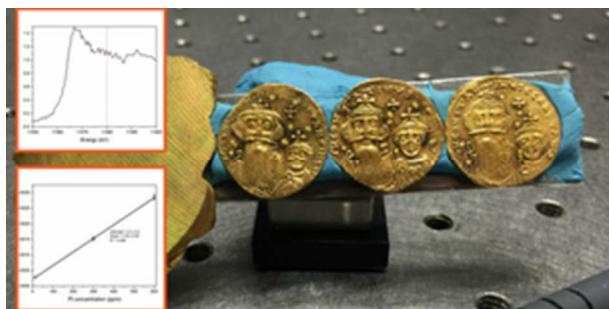


Figure 8. Pt distribution in selected raised regions of the imprinted side of Coin #2. Each map is (400 μm x 400 μm). The relative platinum concentrations are represented using a colour scale from white (highest Pt) to black (lowest Pt). The variation in colour reflects the standard deviations reported in Table 2. Maps 3 and 4 show Pt hotspots.



A non-destructive SR-WD-XRF method for quickly measuring Pt in large sample suites of ancient Roman gold coins.